

# Influence of the concentration of $\text{Sb}_2\text{O}_3$ on the electrical properties of $\text{SnO}_2$ varistors

J. R. Ciórcero · S. A. Pianaro · G. Bacci ·  
A. J. Zara · S. M. Tebcherani · E. Longo

Received: 5 May 2010 / Accepted: 11 August 2010 / Published online: 28 August 2010  
© Springer Science+Business Media, LLC 2010

**Abstract** Varistors are electronic materials with non-ohmic behavior. In traditional  $\text{SnO}_2$  varistors,  $\text{CoO}$  acts as a densifying agent,  $\text{Nb}_2\text{O}_5$  increases the electrical conductivity of  $\text{SnO}_2$  grains, and  $\text{Cr}_2\text{O}_3$  produces a more uniform microstructure and acts as an oxygen retaining agent at the grain boundaries. The present work involved a systematic study of the substitution of  $\text{Nb}_2\text{O}_5$  for  $\text{Sb}_2\text{O}_3$  in the composition of a ternary varistor system. The compositions were prepared by conventional wet ceramic processing using deionized water, and the resulting slips were dried by spray-drying. Pellets were produced under a pressure of 330 MPa and sintered at 1,350 °C for 2 h. Similar to the behavior of  $\text{Nb}_2\text{O}_5$ , increasing the concentration of  $\text{Sb}_2\text{O}_3$  reduced the nonlinear behavior of the ceramic and its breakdown electric field while increasing its leakage current. The samples' microstructure showed greater porosity, suggesting that higher concentrations of  $\text{Sb}_2\text{O}_3$  reduce the sintering rate, probably in response to the higher concentration of tin vacancies in the structure.

## 1 Introduction

Varistors are generally polycrystalline ceramic materials with a microstructure composed of conductive grains surrounded by insulating grain boundaries. Schottky-type potential barriers are formed at these interfaces and are responsible for the nonohmic behavior of varistors. The nonlinearity between the current and the electrical potential of varistors is given by:  $I = K \cdot V^\alpha$ , where  $I$  is the current,  $V$  is the electrical potential,  $K$  is a constant related to the microstructure of the material, and  $\alpha$  is the coefficient of nonlinearity [1]. A  $\text{SnO}_2$ -based ceramic system with a high nonlinear  $I \times V$  characteristic presents properties that are very similar to those of traditional  $\text{ZnO}$  varistors [2], but with a few advantages, such as a simpler microstructure composed of a monophasic system, low concentrations of dopants required to obtain good nonlinear properties, and greater resistance to electrical degradation [3–6].

The  $\text{SnO}_2$  is an  $n$ -type semiconductor with high electron mobility and a tetragonal crystalline structure [7]. It presents low densification, but, in the presence of dopants with an electrical charge of lower valence, it may reach densities approaching the theoretical density of  $\text{SnO}_2$  [8–10]. In addition to densifying oxides, the formation of the varistor's microstructure and electrical properties are highly dependent on the chemical composition, processing technique, sintering conditions and thermal treatments in oxidizing and reducing atmospheres [11–28]. The importance of thermal treatment in oxygen atmosphere to recover the non-ohmic properties of  $\text{ZnO}$  based varistor after degradation is also related in the literature, thermal treatment at 900 °C for 2 h with oxygen flow allowed to obtain better nonlinear properties compared to the standard sample [29]. In addition to the aforementioned variables, a recent study by Ramirez et al. [30] identified another important variable

---

J. R. Ciórcero · S. A. Pianaro (✉) · G. Bacci · A. J. Zara  
Department of Materials Engineering,  
LIMAC—Interdisciplinary Laboratory of Ceramic Materials,  
UEPG—Ponta Grossa State University, Av. Carlos  
Cavalcante 4748, Ponta Grossa, PR 84030-900, Brazil  
e-mail: sap@uepg.br

S. M. Tebcherani  
Department of Chemistry, LIMAC—Interdisciplinary  
Laboratory of Ceramic Materials, UEPG—Ponta Grossa State  
University, Av. Carlos Cavalcante 4748, Ponta Grossa,  
PR 84030-900, Brazil

E. Longo  
Department of Chemistry, INCTMN—Federal University of São  
Carlos, PO Box 676, São Carlos, SP 84030-900, Brazil

that is crucial when SnO<sub>2</sub> varistors are employed in high currents, e.g., as surge arresters. They found that ceramic samples with a small A/V ratio (2.8 cm<sup>-1</sup>) presented minimal variations in microstructure and, hence, in electrical properties inside blocks. On the other hand, ceramic blocks have a critical A/V value with respect to the predominance of nonohmic properties. A critical value of  $A/V \times 5.0 \text{ cm}^{-1}$  was found. This is the minimum value at which the composition (in mol%) 98.9 SnO<sub>2</sub> + 1.0 CoO + 0.05 Nb<sub>2</sub>O<sub>5</sub> + 0.05 Cr<sub>2</sub>O<sub>3</sub>, SCNcr varistor ceramic has a format that is usable as varistor block. After sintering, blocks with lower A/V ratios present a highly resistive behavior which is associated with the larger number of effective SnO<sub>2</sub> barriers (about 85%) [30, 31]. The high number of electrical barriers in SCNcr system is associated with the basically single phase and homogeneous microstructure when compared with a polyphasic ZnO varistor whereas only 35% were active [32]. The increase in resistivity may be attributed to the relatively low electric conductivity of SnO<sub>2</sub> grains, which causes the upturn region of the varistor to begin early. It was found that increasing the concentration of Nb<sub>2</sub>O<sub>5</sub> did not increase the conductivity of SnO<sub>2</sub> grains. Conversely, it increased the varistor's breakdown voltage due to the increase in porosity, since its density was reduced drastically from 6.44 g/cm<sup>3</sup> (with the addition of 0.4 mol% of Nb<sub>2</sub>O<sub>5</sub>) to 4.53 g/cm<sup>3</sup> (with the addition of 1.5 mol% of Nb<sub>2</sub>O<sub>5</sub>) [13]. Earlier works, which examined the effect of Sb<sub>2</sub>O<sub>3</sub> on the electrical properties of SnO<sub>2</sub> varistors, concluded that it degrades the electrical properties by increasing the leakage current excessively [15, 16]. However, to date no systematic study has been conducted to ascertain the effect of the addition of different concentrations of this oxide on the SnO<sub>2</sub>-CoO system in place of Nb<sub>2</sub>O<sub>5</sub>. Therefore, the purpose of this work was to verify the effect of the addition of different concentrations of Sb<sub>2</sub>O<sub>3</sub> (0.05–0.5% in mol) to the SnO<sub>2</sub>-CoO system, as well as to characterize the electrical and microstructural properties of the various resulting ceramic systems.

## 2 Experimental

The following raw materials were used: SnO<sub>2</sub> (CESBRA), CO<sub>3</sub>O<sub>4</sub> (RIEDEL), and Sb<sub>2</sub>O<sub>3</sub> (VETEC). The four formulations from the system (99.00–x)% SnO<sub>2</sub> + 1.00% CO<sub>3</sub>O<sub>4</sub> + x% Sb<sub>2</sub>O<sub>3</sub> (x = 0.05; 0.10; 0.30; 0.50% in mol) called respectively for SCSb0.05, SCSb0.10, SCSb0.30 and SCSb0.50, were homogenized in a wet ball mill for 6 h, using zirconium balls and high-density polyethylene jars. A polyvinyl alcohol and ethylene glycol solution in a proportion of 3% in mass was used as a plasticizer. The dispersant used was 0.3% of ammonium polyacrylate (PAA-NH<sub>4</sub><sup>+</sup>) in

relation to the dry mass. The resulting suspensions were dried by spray dryer atomization (B-290 mini spray dryer) to obtain the granules, whose morphology was then characterized by scanning electron microscopy (SEM) (SHIMADZU). The granulated compositions were compacted uniaxially under a pressure of 330 MPa in an automatic hydraulic press (Nannetti Faenza-Italia), forming compacts of cylindrical geometry with 1.0 cm of diameter and 0.19 cm of thickness. The resulting compacts were oven-dried at 110 °C for 2 h and then sintered at 1,350 °C for 2 h, and subsequently cooled at a rate of 180 °C/h. To eliminate surface irregularities, the samples were sandpapered using silicon carbide grit 400 sandpaper. The geometrical density of these samples after sintering was also calculated. In preparation for the electrical characterization, the samples' surfaces were gold sputter-coated and current–voltage characteristic curves were obtained using a voltage-source meter unit Keithley 237). For the SEM characterization, due to the high resistance of SnO<sub>2</sub> to chemical attack, the samples were sandpapered, polished and heat-treated 50 °C below the sintering temperature to reveal the microstructure. To aid in the identification of possible ceramic phases, samples heat-treated in the same sintering conditions were analyzed by X-ray diffraction (SHIMADZU XRD 6000) using the powder method.

## 3 Results and discussion

The micrographs in Fig. 1 show the granules of atomized powder. In Fig. 1a and b, note the very heterogeneous distribution of these granules. Figure 1c highlights the primary particles that make up these granules, whose sizes are nanometric.

All the systems under study presented a nonlinear  $J \times E$  behavior (Fig. 2). The graph in Fig. 3 indicates the characteristic physical parameters of the varistors obtained from the curves shown in Fig. 2, i.e., nonlinearity coefficient  $\alpha$ , breakdown electric field  $E_r$  (obtained from the electric field equivalent to 1 mA/cm<sup>2</sup> of current density) and leakage current  $I_f$  (obtained for a value of current equivalent to 85% of  $E_r$ ).

As can be seen in Fig. 3, increasing the concentration of antimony oxide (Sb<sub>2</sub>O<sub>3</sub>) led to an increase of leakage current and decrease of the coefficient of nonlinearity and of the breakdown electric field.

Varistors with high leakage current usually present low values of  $\alpha$ . This behavior is directly associated with the low electrical resistivity at the grain boundaries of the ceramic. In other words, the height of the potential barrier associated to the electronic defects at the grain boundaries is relatively low, so the electrons need low activation energy to overcome this barrier. Obviously, the nature and

**Fig. 1** SEM micrographs with different magnifications, showing the characteristics of the granules of spray-dryer atomized powder. **a** 600× magnification; **b** 2,400× magnification; and **c** 24,000× magnification

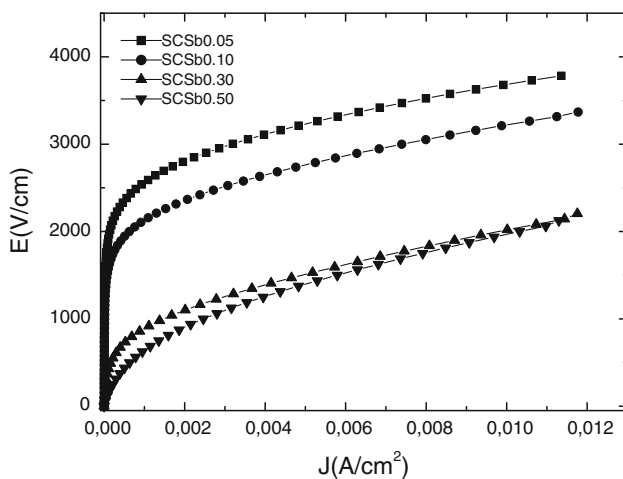
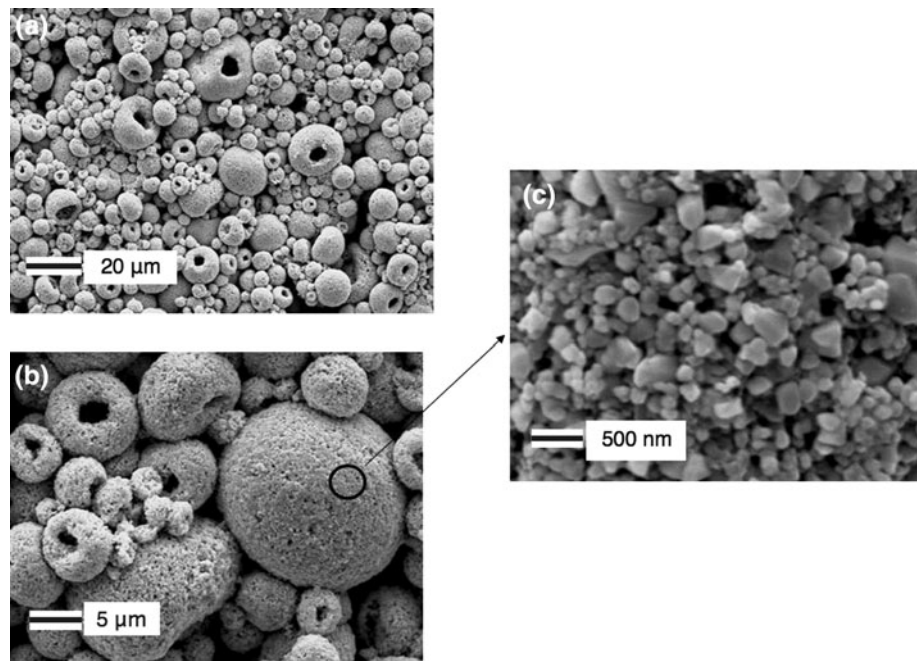


**Fig. 2** Electrical characterization  $J \times E$  of the varistors with different concentrations of  $Sb_2O_3$  in the system  $(99.00-x)\% SnO_2 + 1.00\% Co_3O_4 + x\% Sb_2O_3$  in mol for  $x = 0.05$  (SCSb0.05);  $x = 0.10$  (SCSb0.10);  $x = 0.30$  (SCSb0.30);  $x = 0.50$  (SCSb0.50)

concentration of dopants act to modulate these electrical barriers. The addition of just 0.05% of  $Sb_2O_3$  sufficed to give the ceramic varistor properties, since the  $99.00\%SnO_2 + 1.00\%Co_3O_4$  system proved to be highly resistive [3]. This behavior was very similar to that found in the  $SnO_2-CoO-0.05\%Nb_2O_5$  system studied previously [3], although the respective values of  $\alpha$  and  $E_r$  also presented differences, i.e., 8.0 and 1,800 V/cm for the  $SnO_2-CoO-0.05\%Nb_2O_5$  system and 6.1 and 2,600 V/cm for the  $SnO_2-CoO-0.05\%Sb_2O_3$  system of this work.

Figure 4 shows the X-ray diffractograms and Fig. 5 the SEM micrographs (backscattered electrons) of the systems under study. The results obtained here indicated that:

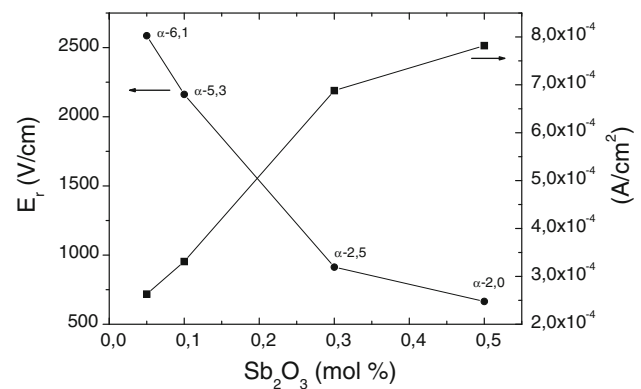


**Fig. 3** Physical parameters of the varistors obtained from the characteristic  $J \times E$  curve for different concentrations of  $Sb_2O_3$  in the system  $(99.0-x)\% SnO_2 + 1.0\% Co_3O_4 + x\% Sb_2O_3$  in mol ( $x = 0.05; 0.1; 0.3; 0.5\%$ )

- Based on the cards of the JCPDS (Joint Committee on Powder Diffraction Standards), all the systems were monophasic, and the phase relating to  $SnO_2$  (cassiterite, card no. 72-1147) was identified.
- With the increase in the  $Sb_2O_3$  concentration, there was a decrease in grain size and an increase in porosity, and this increase was more evident at concentrations exceeding 0.1% in mol.

Based on these observations, it is reasonable to suppose that  $Sb_2O_3$  in concentrations exceeding 0.1% in mol reduces the material’s densification rate. Although the grain size was reduced, no increase was found in the varistor’s breakdown electric field, since  $E_r$  is inversely proportional to grain size. In fact, what occurred was a decrease of the values of  $E_r$ , which may be explained by the

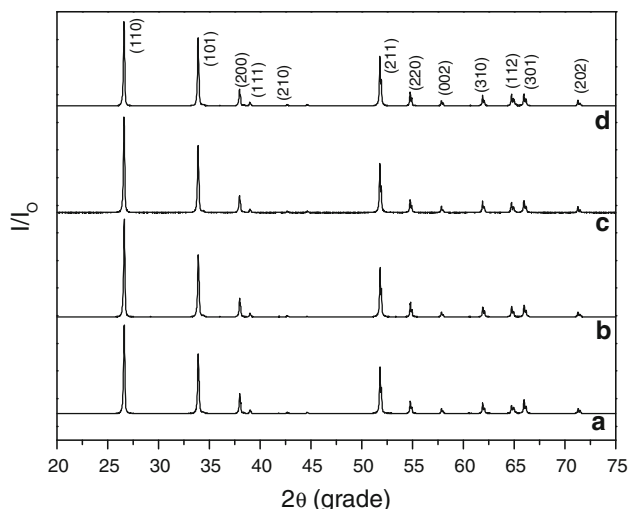
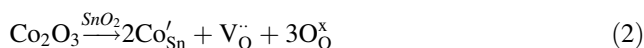


**Fig. 4** X-ray diffractogram of the samples sintered at 1,350 °C/2 h: **a** SCSb0.05, **b** SCSb0.10, **c** SCSb0.30, **d** SCSb0.50

association of two factors: (a) reduction of the number of effective electrical barriers due to porosity, and (b) higher concentration of  $\text{Sb}^{5+}$  close to the interface (barrier width), which, upon substituting  $\text{Sn}^{4+}$  in this region, increases the conductivity of the grain boundary, causing a decrease in the value of  $v_b$  (barrier voltage). According to Li et al. [33] who investigated Sb-doped  $\text{SnO}_2$  using first-principle calculations based on the density functional theory, when one of the 16 Sn atoms in the  $\text{SnO}_2$  supercell is replaced by one Sb atom, the Fermi level moves into the conduction band

and the compound displays metallic characteristics in the electronic band structure.

A correlation can be identified between the microstructure and the electrical properties as a function of the chemical composition, considering the solid state reactions between  $\text{SnO}_2$  and dopants during sintering. It is known from previous studies that  $\text{SnO}_2$  in the pure state presents little or no densification when it is sintered; however, dopants with a +2 load promote its densification. When 1.0 mol% of CoO is added to  $\text{SnO}_2$  [12], the following solid state reaction (Kröger-Vink notation) occurs during sintering:



Thus, the formation of oxygen vacancies produced in the 1 and 2 reactions facilitate diffusion through the  $\text{SnO}_2$  network, promoting its densification, and relative densities of close to 98% of the theoretical density of  $\text{SnO}_2$  may be reached [3]. When  $\text{Sb}_2\text{O}_3$  was added to the binary system  $\text{SnO}_2\text{--Co}_3\text{O}_4$  in concentrations of more than 0.1% in mol, a marked reduction was observed in the density of the samples, forming more porous microstructures as its concentration in the composition increased. Since the theoretical density of  $\text{SnO}_2$  is 6.95 g/cm<sup>3</sup>, the systems under study, SCSb0.05, SCSb0.1, SCSb0.3, and SCSb0.5,

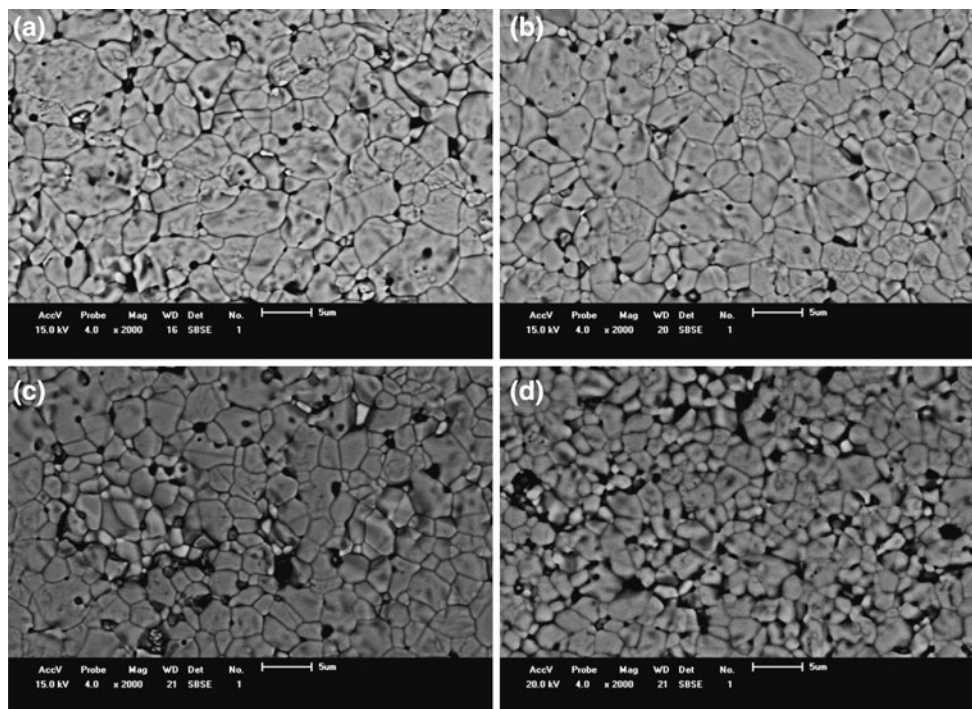
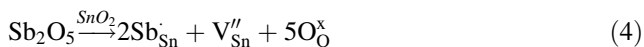


**Fig. 5** SEM micrograph of the systems: **a** SCSb0.05, **b** SCSb0.10, **c** SCSb0.30, **d** SCSb0.50

reached 90.4, 90.8, 84.8, and 83.7% of the theoretical density, respectively.

The following reactions are proposed, considering sintering in an ambient atmosphere:



Unlike reactions 1 and 2, reaction 4 leads to the formation of tin vacancies, i.e., loss of metal in the network, reducing the densification rate and leading to the formation of more porous microstructures, as can be observed in Fig. 5. The higher the concentration of  $\text{Sb}^{5+}$  in substitution of  $\text{SnO}_2$  the higher the concentration of tin vacancies, and hence, the lower the density of the varistor.

#### 4 Conclusions

The conclusions drawn from this work are that  $\text{Sb}_2\text{O}_3$  can be used as a substitute of  $\text{Nb}_2\text{O}_5$  in the proportion of 0.05 mol% in the composition. At higher concentrations, its effect was deleterious because it led to an excessive increase in the current, diminishing the varistor's nonlinearity coefficient. Another characteristic observed at concentrations above 0.1% was the decrease of the breakdown electric field due to the destruction of the grain-grain contacts in the more porous microstructures. This decrease in density as a function of the  $\text{Sb}_2\text{O}_3$  concentration may be associated with increase in the concentration of tin vacancies due to the formation of  $\text{Sb}^{5+}$  solid solution in the  $\text{SnO}_2$  network.

**Acknowledgment** The authors acknowledge the financial support of CNPq (Conselho Nacional de Pesquisa – Brazil).

#### References

1. D.R. Clark, *J. Am. Ceram. Soc.* **82**, 485 (1999)
2. S.A. Pianaro, P.R. Bueno, E. Longo, J.A. Varela, *J. Mat. Sci. Lett.* **14**, 692 (1995)
3. P.R. Bueno, J.A. Varela, E. Longo, *J. European, Ceram. Soc.* **28**, 505 (2008)
4. M.A. Ramírez, W. Bassi, P.R. Bueno, E. Longo, J.A. Varela, *J. Phys D:Appl. Phys.* **41**, 12 (2008)
5. Z.Y. Lu, Z.W. Chen, J.Q. Wu, *J. Ceram. Soc. Jap.* **1376**, 851 (2009)
6. M.A. Ramírez, M. Cilense, P.R. Bueno, E. Longo, J.A. Varela, *J. Phys. D:Appl. Phys.* **42**, 1 (2009)
7. Z.M. Jarzebski, J.P. Marton, *J. Electrochem. Soc.:Reviews and News* **123**, 299C (1976)
8. M.K. Paria, H.S. Maiti, *J. Mater. Sci.* **18**, 2101 (1983)
9. T. Kimura, S. Inada, T. Yamaguchi, *J. Mater. Sci.* **24**, 220 (1989)
10. J.A. Varela, O.J. Whitemore, E. Longo, *Ceram.Int.* **6**, 177 (1990)
11. P.R. Bueno, M.M. Oliveira, W.C. Barcelar-Jr, E.R. Leite, E. Longo, *J. Appl. Phys.* **9**, 6007 (2002)
12. Y.J. Wang, J.F. Wang, C.P. Li, H.C. Chen, W.B. Su, W.L. Zhong, P.L. Zhang, L.Y. Zhao, *J. Mat. Sci. Lett.* **20**, 19 (2001)
13. A.V. Gaponov, A.B. Glot, A.I. Ivon, A.M. Chack, G. Jimenez-Santana, *Mater. Sci. Eng. B* **145**, 76 (2007)
14. A. Mosquera, J.E. Rodríguez-Páez, J.A. Varela, P.R. Bueno, *J. Eur. Ceram. Soc.* **27**, 3893 (2007)
15. F.M. Filho, A.Z. Simões, A. Ries, L. Perazolli, E. Longo, J.A. Varela, *Ceram. Int.* **33**, 187 (2007)
16. I.P. Silva, A.Z. Simões, F.M. Filho, E. Longo, J.A. Varela, L. Perazolli, *Mat. Lett.* **62**, 2121 (2007)
17. P.A. Santos, S. Maruchin, G.F. Menegoto, A.J. Zara, S.A. Pianaro, *Mat. Lett.* **60**, 1554 (2006)
18. W. Chun-Ming, W. Jin-Feng, S. Wen-Bin, C. Honh-Cun, W. Chun-Lei, Z. Jia-Liang, Z. Guo-Zhong, Q. Peng, G. Zhi-Gang, M. Bao-Quan, *Mater. Sci. Eng. B* **127**, 112 (2006)
19. R. Parra, J.A. Varela, C.M. Aldao, M.S. Castro, *Ceram. Int.* **31**, 737 (2005)
20. Q. Peng, W. Jin-Feng, S. Wen-Bin, C. Hong-Chun, Z. Guo-Zong, W. Chun-Ming, M. Bao-Quan, *Mater. Chem. Phys.* **92**, 578 (2005)
21. W. Chun-Ming, W. Jin-Feng, W. Chun-Lei, C. Hong-Chun, S. Wen-Bin, Z. Guo-Zhong, Q. Peng, *J. Appl. Phys.* **97**, 126103 (2005)
22. W. Chun-Ming, W. Jin-Feng, C. Hong-Cun, S. Wen-Bin, Z. Guo-Zhong, Q. Peng, M. Bao-Quan, *Solid State Commun.* **132**, 163 (2004)
23. S.R. Dhage, V. Choube, V. Ravi, *Mater. Sci. Eng.* **B110**, 168 (2004)
24. S.A. Pianaro, P.R. Bueno, P. Olivi, E. Longo, J.A. Varela, *J. Mater. Sci. Mater. Eletron.* **9**, 159 (1998)
25. S.A. Pianaro, P.R. Bueno, P. Olivi, E. Longo, J.A. Varela, *J. Mater. Sci. Lett.* **8**, 634 (1997)
26. M.R. Cássia-Santos, V.C. Souza, M.M. Oliveira, F.R. Sensato, W.K. Bacelar, J.W. Gomes, E. Longo, E.R. Leite, J.A. Varela, *Mater. Chem. Phys.* **90**, 1 (2005)
27. A. Dibb, S.M. Tebcherani, W. Lacerda Jr, M. Cilense, J.A. Varela, *J. Mater. Sci.: Mater. Eletron.* **13**, 567 (2002)
28. W.K. Bacelar, M.M. Oliveira, V.C. Souza, E. Longo, E.R. Leite, *J. Mater. Sci.: Mater. Eletron.* **13**, 409 (2002)
29. M.A. Ramirez, A.Z. Simões, P.R. Bueno, M.A. Marquez, M.O. Orlandi, J.A. Varela, *J. Mater. Sci.* **41**, 6221 (2006)
30. M.A. Ramirez, J.F. Fernández, M. De La Rubia, J. de Frutos, P.R. Bueno, E. Longo, J.A. Varela, *J. Mater. Sci: Mater. Electron.* **20**, 49 (2009)
31. J.S. Vasconcelos, N.S.L.S. Vasconcelos, M.O. Orlandi, P.R. Bueno, J.A. Varela, E. Longo, C.M. Barrado, E.R. Leite, *Appl. Phys. Lett.* **89**, 152102 (2006)
32. M.A. Ramírez, W. Bassi, R. Parra, P.R. Bueno, E. Longo, J.A. Varela, *J. Am. Ceram. Soc.* **91**, 7 (2008)
33. Z.Q. Li, Y.L. Lin, X.D. Liu, L.Y. Liu, H. Liu, Q.G. Song, *J. Appl. Phys.* **106**, 083701 (2009)